International Journal of Engineering Research and General Science Volume 13, Issue 1, January-February 2025
ISSN 2091-2730

Quantum Information-Theoretic Analysis Using the Hulthén-Hellmann Potential Model

Olusegun A. Akinde, Eddy S. William*, Etido P. Inyang***, Ituen B. Okon**, Mfoniso U. Aka

*Department of Physics, School of Pure and Applied Sciences, Federal University of Technology, Ikot Abasi, Nigeria;
**Theoretical Physics Group, Department of Physics, University of Uyo;
***Department of Physics, National Open University of Nigeria, Jabi-Abuja, Nigeria.
***Corresponding Author Email:** williameddyphysics@gmail.com; Phone number: 08034490219

Abstract- This study explores Shannon entropy and Fisher information for the Hulthén-Hellmann potential (HHP) in one and three dimensions, building on the foundational work of William et al. (2020) by utilizing the energy equation and wave function. Our analysis revealed notable similarities in high-order features within both position and momentum spaces. Notably, the findings highlighted enhanced precision in predicting particle localization in position space. Additionally, the combined entropies in position and momentum were found to comply with the Berkner-Bialynicki-Birula-Mycieslki inequality. For three-dimensional systems, the Stam-Cramer-Rao inequalities were also satisfied across various eigenstates, based on the calculated Fisher information. A key observation was that a decrease in position space, indicating improved precision in position measurement, was accompanied by an increase in momentum space, reflecting reduced precision in momentum measurement. This inverse relationship demonstrates the complementary nature of uncertainties in position and momentum, a fundamental aspect of quantum mechanics.

Keywords: Hulthén-Hellmann potential; Fisher information; Shannon entropy; Schrödinger equation; Bound state; Berkner-Bialynicki-Birula-Mycieslki inequality; Stam-Cramer-Rao inequality

Introduction

In recent years, researchers have shown increasing interest in exploring quantum information-theoretic measures across various quantum mechanical systems [1]. Quantum information theory provides a framework for understanding and quantifying information by the use of various measures to analyze different quantum mechanical systems [2-5]. The theory is built on the foundations of the Shannon entropy [6] and Fisher information [7] of classical information theory, and it is used to calculate the final quantum limits while accounting for known local fluctuations in density [8,9].

Shannon entropy originally developed by Claude Shannon in classical information theory, measures the uncertainty or information content associated with a random variable. It is adapted to describe the information content of quantum systems, particularly in the context of measurement outcomes [6]. Recently, Shannon entropy has garnered significant attention among many researchers in quantum physics. It is applied to the probability distribution of measurement. When a quantum system is measured, the outcomes follow a certain probability distribution, which can be described using Shannon entropy. This is particularly relevant when considering the classical information that can be extracted from a quantum system after a measurement [3]. In quantum communication protocols, Shannon entropy helps quantify the amount of classical information that can be transmitted after a quantum measurement. It also plays a role in analyzing the efficiency of quantum encoding schemes [10]. Additionally, Shannon entropy finds applications in data analysis and pattern recognition, machine learning [11], security and cryptography [12]. The Shannon entropy of the measurement outcomes provides a measure of the uncertainty or information gained from the quantum measurement. A higher entropy indicates a higher level of uncertainty in the measurement outcomes, whereas a lower entropy suggests more predictable outcomes [13].

Note- This Manuscript was Submitted on December 20th 2024, Accepted on January 15th 2025 and Published on February 5th 2025

Shannon entropy serves as a precise and quantifiable metric for uncertainty and information content, establishing itself as an essential tool for analyzing, modeling, and optimizing systems and processes that involve information [14]. The Shannon entropic uncertainty relation in position and momentum spaces satisfied the Bialynicki-Birula and Mycielski (BBM) [15,16] inequality relation which is a generalized Heisenberg uncertainty principle of quantum mechanics and it is expressed as

$$S_T = S_r + S_p \geq D\left(1+2\ln\pi\right), \qquad (1)$$

where, D represents the spatial dimension, S_r denotes the Shannon entropy in the coordinate space, S_p represents the corresponding Shannon entropy in the momentum space, and S_T is the Shannon entropy sum. They are defined as follows [17-19]:

$$\begin{aligned} S_r &= -\int \left|\Psi\left(r,\theta,\varphi\right)\right|^2 \ln\left|\Psi\left(r,\theta,\varphi\right)\right|^2 d^3r, \\ S_p &= -\int \left|\varphi\left(p\right)\right|^2 \ln\left|\varphi\left(p\right)\right|^2 d^3p, \end{aligned} \qquad (2)$$

where $d^3r = r^2 dr d\Omega, d^3p = p^2 \sin\theta d\Omega, and\ d\Omega = \sin\theta d\theta d\varphi$ is the solid angle with $\Psi\left(r,\theta,\varphi\right)$ being the normalized wave function in the special coordinate. Also, $\rho\left(r\right) = \left|\Psi\left(r,\theta,\varphi\right)\right|^2$ is the probability density in the spatial co-ordinate, $\rho\left(p\right) = \left|\phi\left(p\right)\right|^2$ is the probability density in the momentum space and $\phi\left(p\right)$ is the associated normalized Fourier transform [15].

On the other hand, Fisher information is a critical concept in both statistics and information theory, providing a quantitative measure of the information content in data regarding an unknown parameter upon which the probability depends [20, 21]. While entropy measures the uncertainty in a random variable, Fisher's information can be seen as measuring the sensitivity of this uncertainty to changes in the parameter. In this sense, Fisher information provides a bridge between the statistical properties of estimators and the informational content of the data [22]. Fisher information provides insights into the precision with which a parameter can be estimated based on the observed data. It is particularly important in the context of the Cramér-Rao bound, which establishes a lower bound on the variance of unbiased estimators of a parameter. The Cramér-Rao bound is inversely proportional to the Fisher information, implying that higher Fisher information leads to lower variance of the estimator, thus enabling more precise estimates [13]. Its relevance spans across various domains, including parameter estimation, signal processing and machine learning, underscoring its importance in the efficient processing and interpretation of information. It is represented in both coordinate and momentum spaces as [23]

$$\begin{aligned} I_r &= \int \rho\left(r\right)\left|\nabla\rho\left(r\right)\right|^2 d^3r, \\ I_r &= \int \phi\left(p\right)\left|\nabla\phi\left(p\right)\right|^2 d^3p. \end{aligned} \qquad (3)$$

Unlike, the Shannon entropy that satisfied the BBM inequality, the Fisher information fulfills the Stam inequalities $I_r \leq 4\left\langle p^2\right\rangle; I_p \leq 4\left\langle r^2\right\rangle$ [24], and the Cramer–Rao inequalities $I_r \geq \frac{9}{\left\langle r^2\right\rangle}; I_p \geq \frac{9}{\left\langle p^2\right\rangle}$ [25]. In general, for any central potential model with an arbitrary angular momentum quantum number, the two products of the Fisher information are required to satisfy the relation [26].

$$I_r I_p \geq 4\left\langle r^2 \right\rangle \left\langle p^2 \right\rangle \left[2 - \frac{2l+1}{l(l+1)} |m| \right]^2, \tag{4}$$

where the magnetic quantum number $m = 0, \pm 1, \pm 2 \pm \ldots$ With the definitions of Eqs. (1–3), we can define the Shannon power in position and momentum space as $J_r = \frac{1}{2\pi e} e^{\frac{2S_r}{D}}$, $J_p = \frac{1}{2\pi e} e^{\frac{2S_p}{D}}$ and the Fisher–Shannon product in position and momentum spaces as $P_r = \frac{I_r J_r}{D}, P_p = \frac{I_p J_p}{D}$ which must satisfy the relation $P = P_r P_p > 1$ [27]. Fisher information is considered a local measure because it is sensitive to changes in local density. Studies on information-theoretic measures of probability distributions in quantum mechanical states, both in position and momentum, have shown that reduced uncertainty leads to increased accuracy in estimating particle localization [28].

Quantum information theory has demonstrated remarkable utility across various fields, including quantum physics, where it is employed to study phenomena such as quantum steering [29], quantum entanglement [30], quantum revivals [31], quantum communication [32], and atomic ionization properties [33]. In wave mechanics, on the other hand, solving the eigenfunctions of the Schrödinger equation under a potential energy barrier is crucial, as the entropic functionals are derived from the probability densities in position and momentum spaces [34]. Quantum information measures play a crucial role in understanding the behavior and characteristics of quantum systems. In the context of a 2-dimensional Schrödinger equation under the influence of solvable potentials, combined with magnetic and Aharonov–Bohm (AB) flux fields, these measures provide insights into the quantum states' complexity, coherence, and entanglement properties and have been studied by many authors. The incorporation of magnetic and Aharonov-Bohm flux fields is particularly significant in this context because, the eigenvalues and eigenfunctions are influenced by these fields, leading to a shift in the energy eigenvalue and eigenfunctions, breaking the degeneracy and modifying the results when compared to flat space [35-37]. Quantum Fisher Information (QFI) extends classical Fisher information to quantum systems and is crucial in quantum estimation theory. QFI provides the ultimate precision limit in estimating a parameter encoded in a quantum state.

Different potentials such as Harmonic Oscillator Potential, Coulomb potential, Double-Well Potential, Pöschl-Teller Potential, Kronig-Penney Potential, Morse potential, and others are applied in quantum information theory to model and explore the behavior of quantum systems under various conditions. These potentials provide insights into quantum coherence, entanglement, state evolution, and the effectiveness of quantum computations. Understanding these potentials is essential for advancing quantum technologies, including quantum computation, quantum communication, and quantum sensing [46-50]. The potentials we have selected for our study is the Hulthén-Hellmann potential (HHP). The analytical solutions of the Schrödinger equation (SE) with the Hulthén-Hellmann potential are important for understanding quantum systems where both short-range and long-range interactions are present. The Hulthén-Hellmann potential combines the characteristics of the Hulthén potential, which models short-range interactions, and the Hellmann potential, which includes Coulomb and screened Coulomb (Yukawa-like) terms making it useful for systems with competing forces where the electron-electron and electron-nucleus interactions need to be modeled accurately. These potentials are widely used in atomic, molecular, and nuclear physics to model interactions between particles. The aim of this work is to extend the study carried out by William et al [51] on the analytical solutions of the SE with the Hulthén-Hellmann potential to Shannon entropy and information theoretic-measures in higher dimensions. It is interesting to note that no study has been carried out with this potential in this area of research. The potential is of the form

$$V(r)=-\frac{\Lambda_1 e^{-\alpha r}}{1-e^{-\alpha r}}-\frac{\Lambda_2}{r}+\frac{\Lambda_3 e^{-\alpha r}}{r} \tag{5}$$

where r represents the inter-nuclear distance; and η_1, η_2, and η_3 are the strengths of Hulthén, Coulomb, and Yukawa potentials, respectively, and α is the screening parameter. This potential has been studied by some authors in few areas of physics. For instance, Akpan et al [52], studied the mass spectra of heavy mesons. Duan et al [53] studied the optical absorption coefficients and refractive index changes in the GaAs/Ga1−x AlxAs spherical quantum dots. Chang [54] calculated the third-harmonic generation related to the electronic state of GaAs/$Al_{0.3}Ga_{0.7}$As spherical quantum dot. Chang and Li [55] studied theoretically the nonlinear optical properties of quantum dots of GaAs/$Al_\eta Ga_{1-\eta}$As. Hence, our aim is to investigate the information metric with the Hulthén-Hellmann potential (HHP) which have not been explored to the best of our knowledge .The energy eigenvalues of the HHP and the normalized wavefunctions were obtained using the Nikiforov–Uvarov (NU) method (William et al 2020) and is presented as

$$E_{nl}=\frac{\alpha^2\hbar^2 l(l+1)}{2\mu}-\eta_2\alpha-\frac{\alpha^2\hbar^2}{8\mu}\left[\frac{(n+l+1)^2+\frac{2\mu\eta_3}{\alpha\hbar^2}-\frac{2\mu\eta_2}{\alpha\hbar^2}-\frac{2\mu\eta_1}{\alpha^2\hbar^2}+l(l+1)}{(n+l+1)}\right]^2, \tag{6}$$

Using the wavefunction $\phi(s)$ and weight function $\rho(s)$ given as

$$\phi(s)=s^{\sqrt{\omega_3}}(1-s)^{\left(\frac{1}{2}+\sqrt{\omega_3+\omega_2+\omega_1}\right)}, \tag{7}$$

$$\rho(s)=s^{2\sqrt{\omega_3}}(1-s)^{2\sqrt{\omega_3+\omega_2+\omega_1}}. \tag{8}$$

The wavefunction is written as

$$\psi_{nl}(s)=\left[\frac{n!2\sqrt{\omega_3}\;\alpha\;\Gamma\left(2\sqrt{\omega_3}+\sqrt{4\omega_3+4\omega_2+4\omega_1}+n+2\right)}{2\Gamma\left(2\sqrt{\omega_3}+n+1\right)\Gamma\left(\sqrt{4\omega_3+4\omega_2+4\omega_1}+n+2\right)}\right]^{\frac{1}{2}} s^{\sqrt{\omega_3}}(1-s)^{\left(\frac{1}{2}+\sqrt{\omega_3+\omega_2+\omega_1}\right)} P_n^{\left(2\sqrt{\omega_3},2\sqrt{\omega_3+\omega_2+\omega_1}\right)}(1-2s), \tag{9}$$

where

$$s=e^{-\alpha r}, \tag{10}$$

$$\left.\begin{aligned}\omega_1&=\left(\frac{1}{4}-\frac{2\mu E_{nl}}{\alpha^2\hbar^2}+\frac{2\mu\Lambda_1}{\alpha^2\hbar^2}-\frac{2\mu\Lambda_3}{\alpha\hbar^2}\right),\quad \omega_2=\left(-\frac{4\mu E_{nl}}{\alpha^2\hbar^2}+\frac{2\mu\Lambda_1}{\alpha^2\hbar^2}-\frac{2\mu\Lambda_2}{\alpha\hbar^2}-\frac{2\mu\Lambda_3}{\alpha\hbar^2}\right),\\ \omega_3&=\left(-\frac{2\mu E_{nl}}{\alpha^2\hbar^2}-\frac{2\mu\Lambda_2}{\alpha\hbar^2}+l(l+1)\right),\omega_1+\omega_2+\omega_3=\frac{1}{4}-\frac{8\mu E_{nl}}{\alpha^2\hbar^2}+\frac{4\mu\Lambda_1}{\alpha^2\hbar^2}-\frac{4\mu\Lambda_2}{\alpha\hbar^2}-\frac{4\mu\Lambda_3}{\alpha\hbar^2}+l(l+1)\end{aligned}\right\}. \tag{11}$$

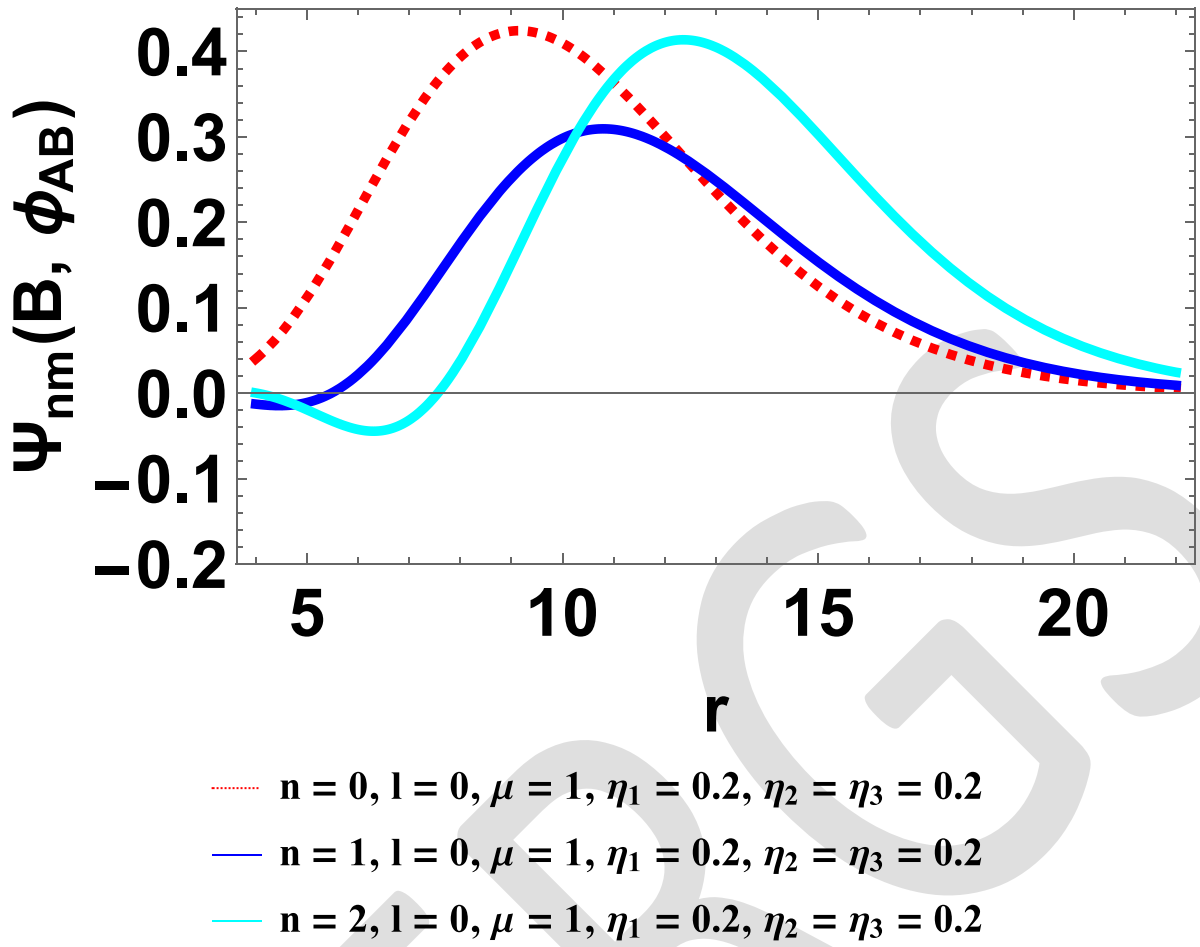

Fig 1: Plots of wave function versus internuclear distance of HHP for various quantum numbers

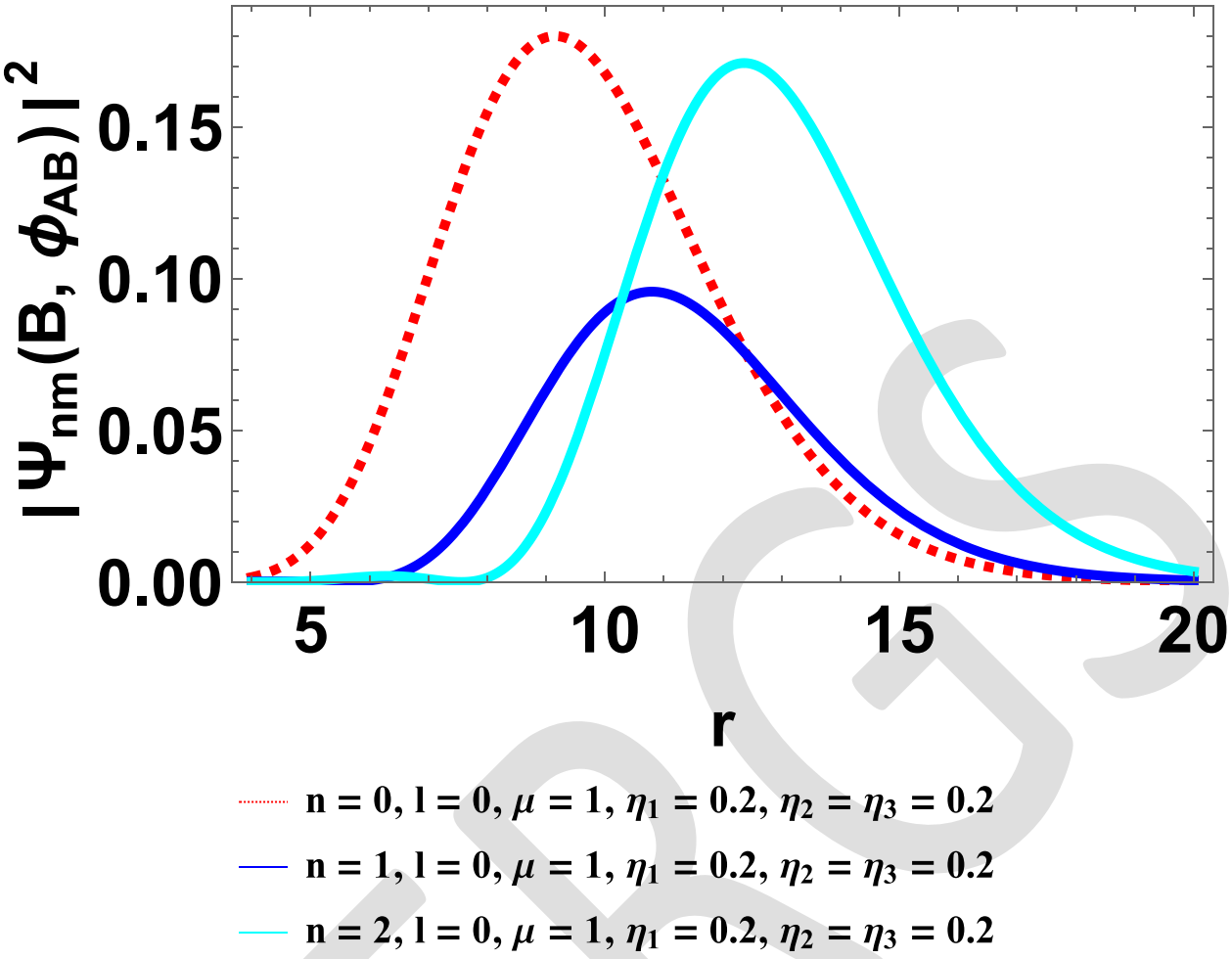

Fig 2: Plots of probability density versus internuclear distance of HHP for various quantum numbers

2. Shannon entropy and Fisher information-theoretic measures in 1 and 3 Ds

In the present consideration, we present the results of the Shannon entropy and Fisher information entropy of this potential in higher dimensions.

Table 1. Numerical results of Shannon entropy in 1-D for two low-lying states $S_p + S_\gamma = S_T \geq D(1+\ln\pi) \geq 2.14473$

n	α	S_p	S_γ	S_T	n	S_p	S_γ	S_T
0	0.1	2.2235	0.0372922	2.18621	1	2.46228	0.399604	2.86188
	0.2	1.91325	0.308884	2.22213		2.11772	0.789955	2.90767
	0.3	1.73959	0.513014	2.25261		1.90628	1.00938	2.91566
	0.4	1.61636	0.661359	2.27772		1.74196	1.17149	2.91345
	0.5	1.51644	0.781413	2.29785		1.60035	1.30923	2.90958
	0.6	1.42828	0.885350	2.31363		1.47294	1.43329	2.90623
	0.7	1.34650	0.979280	2.32578		1.35635	1.54737	2.90371
	0.8	1.26863	1.066390	2.33502		1.24892	1.65299	2.90191
	0.9	1.19364	1.148360	2.34200		1.14958	1.75105	2.90064
	1.0	1.12119	1.226060	2.34725		1.05747	1.84226	2.89973
	1.1	1.05122	1.299970	2.35119		0.971807	1.92728	2.89909
	1.2	0.983755	1.370390	2.35414		0.891918	2.00671	2.89863
	1.3	0.918828	1.437530	2.35635		0.817194	2.08111	2.89830
	1.4	0.856438	1.501570	2.35801		0.747094	2.15097	2.89807
	1.5	0.796549	1.562700	2.35925		0.681146	2.21675	2.89790
	1.6	0.739096	1.62107	2.36017		0.618933	2.27885	2.89778
	1.7	0.683989	1.67685	2.36084		0.560091	2.33761	2.8977
	1.8	0.631125	1.73021	2.36133		0.504302	2.39334	2.89764
	1.9	0.580391	1.78129	2.36192		0.451285	2.44632	2.89761
	2.0	0.531675	1.83025	2.36192		0.400795	2.49679	2.89759

Table 2. Numerical results of Shannon entropy in 3-D for two low-lying states $\left(S_p + S_\gamma = S_T \geq D(1+\ln\pi) \geq 6.43419\right)$

n	α	S_p	S_γ	S_T	n	S_p	S_γ	S_T
0	0.1	238.428	0.06433	238.493	1	351.863	0.06433	351.928
	0.2	68.8769	0.19386	69.0708		114.014	0.19533	114.209
	0.3	36.3621	0.37162	36.7337		61.1039	0.37630	61.4802
	0.4	24.0451	0.59922	24.6443		38.7166	0.61000	39.3266
	0.5	17.6790	0.87996	18.5589		26.4487	0.90327	27.3520
	0.6	13.7287	1.21705	14.9457		18.8525	1.26394	20.1164
	0.7	10.9836	1.61333	12.5969		13.8356	1.69914	15.5348
	0.8	8.94147	2.07156	11.0130		10.3878	2.21478	12.6026
	0.9	7.36141	2.59453	9.95594		7.94883	2.81560	10.7644
	1.0	6.11114	3.18502	9.29616		6.18269	3.50544	9.68813
	1.1	5.10856	3.84571	8.95427		4.87771	4.28749	9.16520
	1.2	4.29742	4.57913	8.87655		3.89615	5.16440	9.06055
	1.3	3.63667	5.38756	9.02423		3.14599	6.13847	9.28446
	1.4	3.09514	6.27306	9.36820		2.5644	7.21174	9.77614
	1.5	2.64879	7.23746	9.88624		2.10764	8.38600	10.4936
	1.6	2.27877	8.28238	10.5612		1.7447	9.66287	11.4076
	1.7	1.97033	9.40927	11.3796		1.45326	11.0439	12.4971
	1.8	1.71177	10.6194	12.3312		1.21698	12.5303	13.7473
	1.9	1.49385	11.9141	13.4079		1.02374	14.1235	15.1473
	2.0	1.30921	13.2942	14.6035		0.864466	15.8247	16.6891

Table 3. Numerical results of Fisher information in 1-D for two low-lying states $I_p + I_\gamma = I_T \geq 4D^2 \geq 4$

n	α	I_p	I_γ	I_T	n	I_p	I_γ	I_T
0	0.1	0.218764	10.7018	4.09127	1	19.1242	398.783	7626.40
	0.2	0.445009	9.67785	4.30673		10.6386	123.947	1318.63
	0.3	0.686357	6.69035	4.59197		7.88325	67.1369	529.257
	0.4	0.950158	5.16664	4.90913		6.56328	44.9717	295.162
	0.5	1.243120	4.20500	5.22734		5.81762	33.4359	194.517
	0.6	1.571170	3.51554	5.52350		5.35742	26.3188	141.001
	0.7	1.939370	2.98224	5.78365		5.05773	21.4225	108.349
	0.8	2.353000	2.55200	6.00230		4.85549	17.8098	86.4756
	0.9	2.812570	2.19734	6.18018		4.71552	15.0237	70.8445
	1.0	3.323850	1.90187	6.32154		4.61679	12.8137	59.1580
	1.1	3.888000	1.65433	6.43205		4.54616	11.0279	50.1344
	1.2	4.506640	1.44618	6.51742		4.49509	9.56579	42.9991
	1.3	5.180960	1.27058	6.58280		4.45788	8.35661	37.2528
	1.4	5.911850	1.12190	6.63249		4.43065	7.34805	32.5566
	1.5	6.699940	0.99553	6.66998		4.41070	6.50046	28.6716
	1.6	7.545700	0.88766	6.69801		4.39614	5.78319	25.4237
	1.7	8.449480	0.79517	6.71873		4.38558	5.17223	22.6833
	1.8	9.411500	0.71549	6.73379		4.37805	4.64862	20.3519
	1.9	10.43200	0.64652	6.74447		4.37280	4.19722	18.3536
	2.0	11.51100	0.58655	6.75176		4.36930	3.80591	16.6292

Table 4. Numerical results of Fisher information in 3-D for two low-lying states $I_p + I_\gamma = I_T \geq 4D^2 \geq 36$

n	α	I_p	I_γ	I_T	n	I_p	I_γ	I_T
0	0.1	19.1242	398.783	7626.40	1	54.3233	559.227	30379.0
	0.2	10.6386	123.947	1318.63		30.1374	203.562	6134.82
	0.3	7.88325	67.1369	529.257		22.7463	117.266	2667.37
	0.4	6.56328	44.9717	295.162		19.4571	78.9971	1537.05
	0.5	5.81762	33.4359	194.517		17.7323	57.2721	1015.57
	0.6	5.35742	26.3188	141.001		16.7378	43.3503	725.588
	0.7	5.05773	21.4225	108.349		16.1270	33.8146	545.326
	0.8	4.85773	17.8098	86.4756		15.7343	27.0024	424.862
	0.9	4.71552	15.0237	70.8445		15.4729	21.9850	340.173
	1.0	4.61679	12.8137	59.1580		15.2943	18.1985	278.334
	1.1	4.54616	11.0279	50.1344		15.1696	15.2814	231.813
	1.2	4.94509	9.56579	42.9991		15.0812	12.9933	195.955
	1.3	4.45788	8.35661	37.2528		15.0179	11.1700	167.750
	1.4	4.43065	7.34805	32.5566		14.9721	9.69645	145.176
	1.5	4.41070	6.50046	28.6716		14.9389	8.49039	126.837
	1.6	4.39614	5.78319	25.4237		14.9148	7.49198	111.742
	1.7	4.38558	5.17223	22.6833		14.8976	6.65695	99.1725
	1.8	4.37805	4.64862	20.3519		14.8854	5.95204	88.5984
	1.9	4.37280	4.19722	18.3536		14.8770	5.35194	79.6205
	2.0	4.3693	3.80591	16.6292		14.8714	4.8371	71.9345

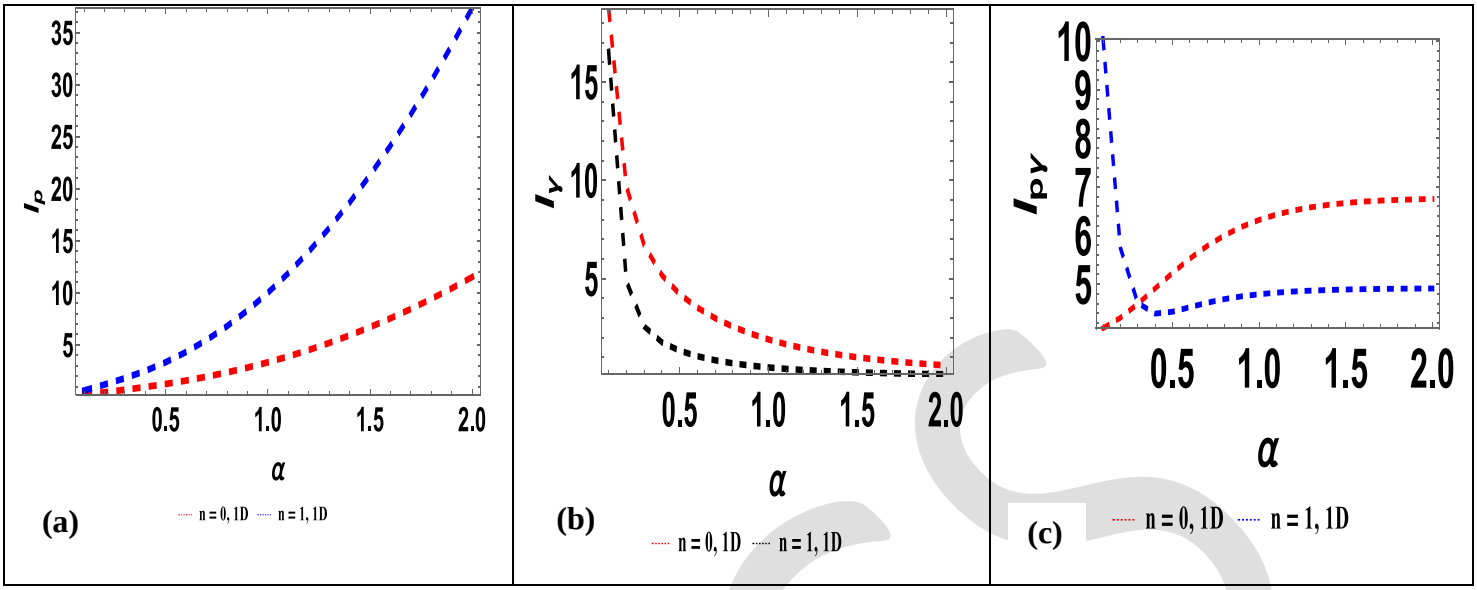

Fig 3: Plots of Fisher in 1D for (a) Position space (b) Momentum space (c) Product space

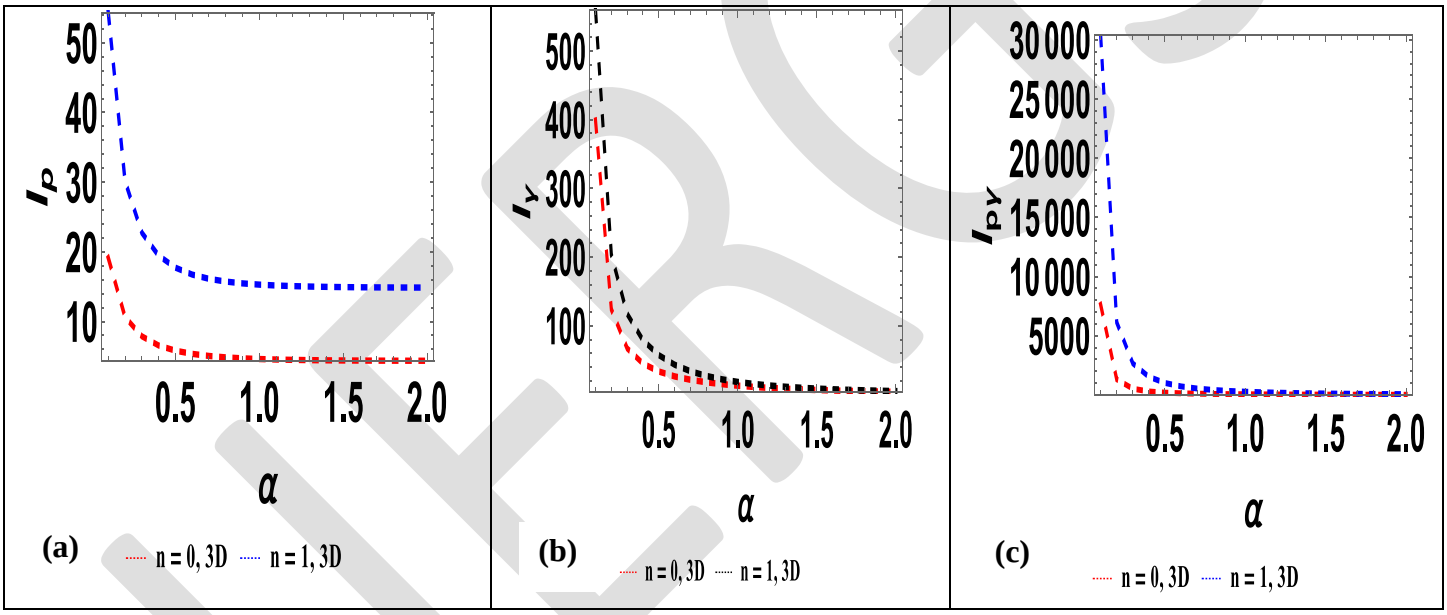

Fig 4: Plots of Fisher in 3D for (a) Position space (b) Momentum space (c) Product space

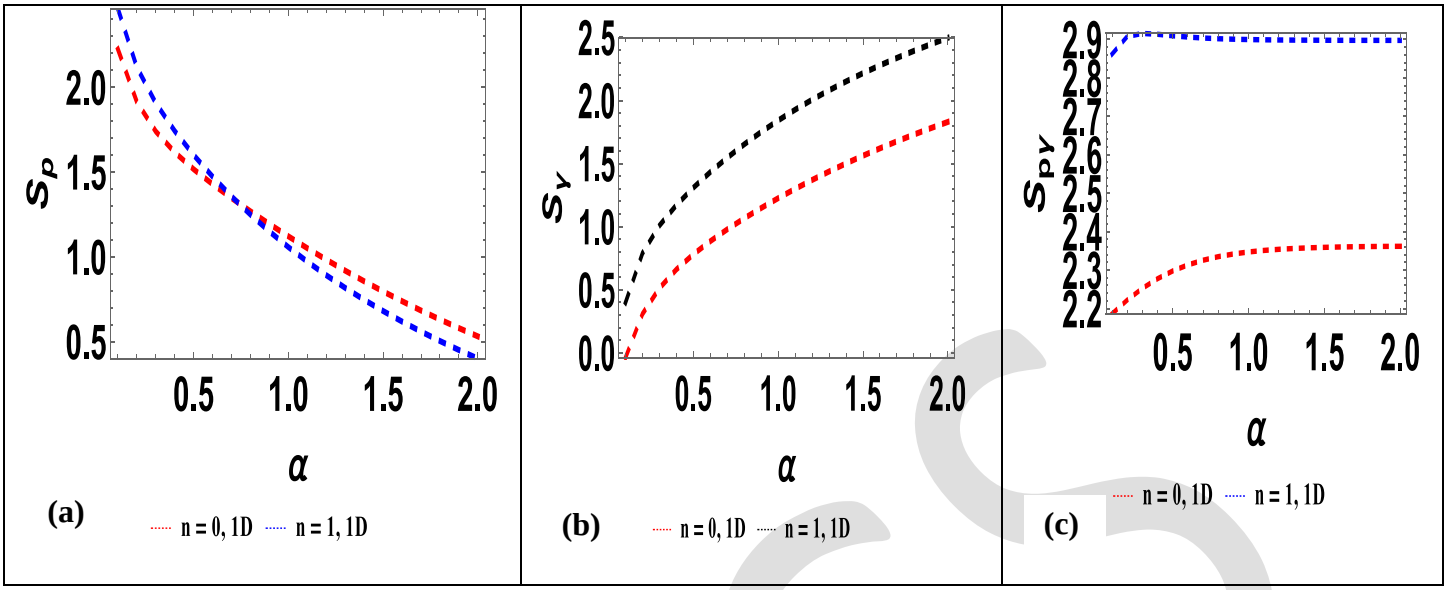

Fig 5: Plots of Shannon in 1D for (a) Position space (b) Momentum space (c) Product space

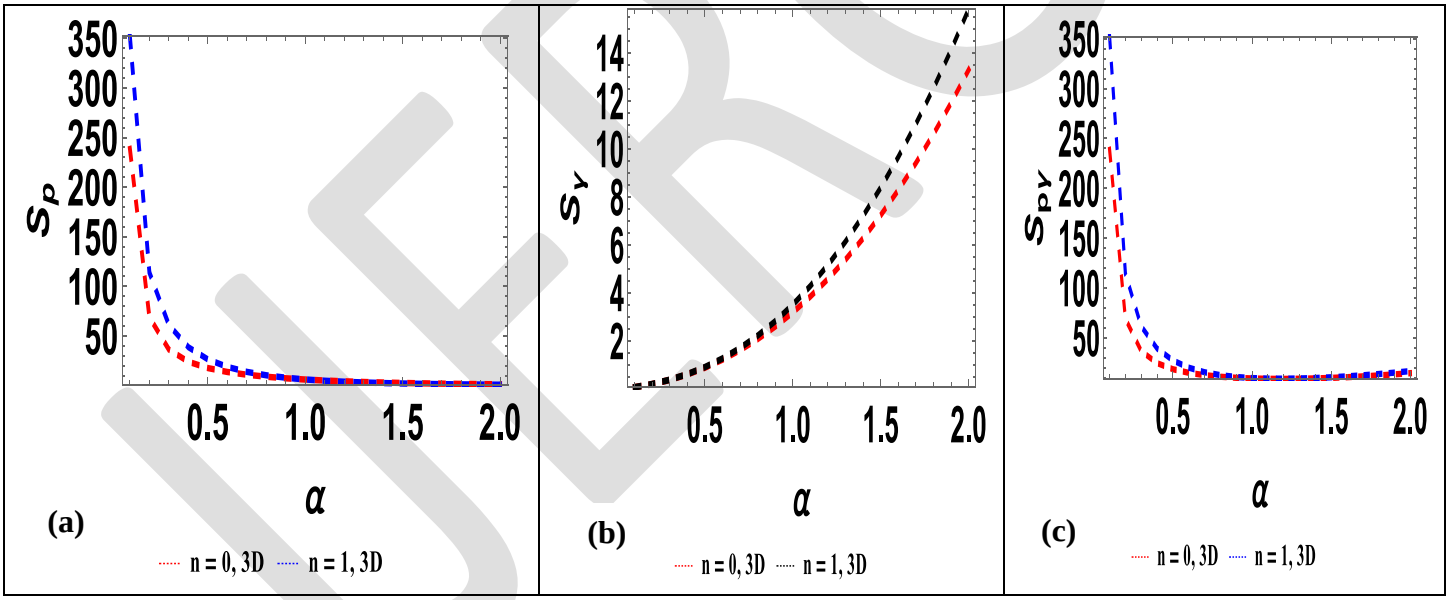

Fig 6: Plots of Shannon in 3D for (a) Position space (b) Momentum space (c) Product space

3. Discussion of the results

In this study, we extend the work of William et al. [51] on the investigation of Fisher information and Shannon entropies in one and three dimensions. **Table 1** presents the one-dimensional ground-state Shannon entropy for various values of the screening parameter (α). As α increases, the entropy in position space decreases, while the entropy in momentum space increases for both the ground and first excited states. This trend highlights how variations in α influence uncertainties in measuring the particle's position and momentum, illustrating the complementary nature of these uncertainties as described by the uncertainty principle and confirming the system's adherence to the BBM inequality of $S_p + S_\gamma = S_T \geq D(1+\ln\pi) \geq 2.14473$. **Table 2** shows the three-dimensional

ground-state Shannon entropy for values of the screening parameter ranging from 0.1 to 2.0. As α increases, the entropy in position space decreases, while the entropy in momentum space increases. The total entropy exceeds 6.43419, satisfying the BBM inequality in three dimensions. This suggests that as the precision in determining the particle's position improves, the precision in determining its momentum diminishes. This balance underscores a fundamental principle of quantum mechanics, highlighting the wave-particle duality and the inherent limitations on precisely measuring conjugate properties such as position and momentum. **Table 3** displays the one-dimensional ground-state Fisher information for various values of the screening parameter. The product of the entropies in position and momentum spaces adheres to the Stam-Cramer-Rao (SCR) inequality for both the ground and first excited states. This adherence implies that in a quantum system, as the precision in measuring the particle's position increases, the precision in measuring its momentum decreases, and vice versa. This reflects the fundamental quantum mechanical principle that a more precise measurement of one property (such as position) results in greater uncertainty in its conjugate property (such as momentum), further emphasizing the constraints imposed by the uncertainty principle. **Table 4** presents the three-dimensional ground-state Fisher information for varying values of the screening parameter. As α increases, the product of the entropies exceeds 36 for both the ground and first excited states. This reflects the quantum relationship between position and momentum measurements, consistent with the uncertainty principle, and satisfies the Stam-Cramer-Rao (SCR) inequality, indicating quantum mechanical limits.

Figures 1 and 2 illustrate the wave function and probability density of the HHP for various principal quantum numbers. As the principal quantum number increases, the wave function exhibits a notable rise in amplitude and complexity. These wave functions display multiple sinusoidal patterns, each corresponding to different quantum states, with the curves intertwining while all other parameters are held constant.

In Figure 2, the probability density plots reveal curves resembling normal distributions with multiple peaks. Each peak corresponds to a distinct quantum state, reflecting the inherent quantization of the system. This progression highlights the intricate relationship between the quantum number and the spatial distribution of the particle. Figure 3(a, b, c) depicts the Fisher information (FI) in position space, momentum space, and their product, plotted in 1D. Fisher information quantifies the amount of information a system's observable carries about a parameter, in this case, the screening parameter. In Fig. 3(a), Fisher information in position space increases with the screening parameter. Physically, this indicates that as the screening becomes more significant, the spatial localization of the wave function becomes sharper, increasing sensitivity to positional variations. In Fig. 3(b), Fisher information in momentum space decreases with the screening parameter. This trend suggests reduced sensitivity in momentum space localization, attributed to the screening effect, which broadens the momentum distribution. In Fig. 3(c), the product of Fisher information in position and momentum spaces shows an exponential decrease with an initial rise for the ground state. The initial rise reflects competing localization effects between position and momentum spaces. Figure 4(a, b, c) presents the Fisher information in 3D for position space, momentum space, and their product. In all cases, an exponential decrease is observed as the screening parameter increases. This trend reflects spatial delocalization induced by screening in higher dimensions, where the wave function spreads more evenly, thereby reducing information density. Figures 5(a, b, c) display Shannon entropy (SE) in 1D as a function of the screening parameter for position space, momentum space, and their sum. Shannon entropy quantifies the uncertainty or spread of the wave function. In Fig. 5(a), Shannon entropy in position space decreases with increasing screening parameter, signifying enhanced spatial localization. Conversely, Fig. 5(b) shows an increase in Shannon entropy in momentum space, indicating broader momentum distribution due to increased screening. In Fig. 5(c), the sum of position and momentum space entropies reflects a similar combined trend, highlighting the interplay between these spaces. Figure 6(a, b, c) extends the analysis of Shannon entropy to 3D for position space, momentum space, and their sum, plotted against the screening parameter. In Fig. 6(a), Shannon entropy in position space decreases with increasing screening parameter, confirming enhanced spatial localization in 3D. In Fig. 6(b), Shannon entropy in momentum space increases, reflecting the broadening of momentum distribution as spatial localization becomes more pronounced. Fig. 6(c) reveals a

decreasing trend in the sum of Shannon entropies for both the ground and first excited states, suggesting that overall uncertainty is more influenced by position space behavior in 3D systems.

Acknowledgements

Olusegun A. Akinde acknowledges the Tertiary Education Trust Fund (TETFUND) of Nigeria for funding this research through the Federal University of Technology, Ikot Abasi with grant number FUTIA/ICR/TETFUND/IBR/AS0064/VOL.1

4.Conclusion

In this research, we build upon the work of William et al. [51]. Our study focuses on analyzing Shannon entropy and Fisher information in both position and momentum spaces in one and three dimensions. We observed that these measures adhere to the Bialynicki-Birula and Mycielski (BBM) inequality as well as the Stam-Cramer-Rao (SCR) inequality across both dimensional frameworks. Moreover, we generated plots of wave functions and probability densities for the HHP, and also 1D and 3D providing a detailed visual representation of the system. The findings revealed a distinct balance: as Fisher information increased in momentum space, it correspondingly decreased in position space as shown in the Tables (1-4). This inverse relationship underscores the fundamental trade-off imposed by the uncertainty principle, which limits the simultaneous precision in measuring conjugate variables. This interplay reflects the inherent balancing act of quantum systems, offering deeper insights into optimizing quantum measurement techniques. Furthermore, the study demonstrates the utility of Fisher information as a robust metric for quantifying quantum uncertainty and enhancing the understanding of measurement sensitivity [56-63].

Funding

This work was supported by the 2022-2023 merged TETFUND INSTITUTION BASED RESEARCH (IBR) with grant number FUTIA/ICR/TETFUND/IBR/AS0064/VOL.1

REFERENCES:

[1] Ikot, A. N., Rampho, G. J., Amadi, P. O., Sithole, M. J., Okorie, U. S., & Lekala, M. I. (2020). Shannon entropy and Fisher information-theoretic measures for Mobius square potential. *European Physical Journal Plus, 135*(503). https://doi.org/10.1140/epjp/s13360-020-00525-2

[2] Omugbe, E., Inyang, E. P., Horchani, R., Eyube, E. S., Onate, C. A., Targema, T. V., ... & Ogundeji, S. O. (2024). The correspondences between variance and information entropies of a particle confined by a q-deformed hyperbolic potential. *Modern Physics Letters A, 39*(31n32), 2450151.

[3] Inyang, E. P., Aouami, A. E. L., Ali, N., Endut, R., Ali, N. R., & Aljunid, S. A. (2024). Information entropies with Varshni-Hellmann potential in higher dimensions. *Physics Open, 20,* 100220.

[4] Omugbe, E., Inyang, E., Jahanshir, A., Onate, C. A., Isonguyo, C. N., Eyube, E. S., ... & Ikot, A. N. (2025). Expectation values and Fisher information-theoretic measures of heavy flavoured mesons. *Journal of the Nigerian Society of Physical Sciences*, 2350-2350.

[5] Inyang, E. P., Nwachukwu, I. M., Ekechukwu, C. C., Ekong, I. B., William, E. S., Lawal, K. M., ... & Oyelami, O. A. (2024). Analytical solution of the class of inversely quadratic Yukawa potential with application to quantum mechanical systems. *Eurasian Physical Technical Journal*, *21*(4 (50)), 118-130.

[6] Shannon, C. E. (1948). A mathematical theory of communication. *Bell System Technical Journal, 27,* 379. https://doi.org/10.1002/j.1538-7305.1948.tb01338.x

[7] Fisher, R. A. (1925). Theory of statistical estimation. *Proceedings of the Cambridge Philosophical Society, 22,* 700. https://doi.org/10.1017/S0305004100009580

[8] Omugbe, E., Osafile, O. E., Okon, I. B., Inyang, E. P., William, E. S., & Jahanshir, A. (2022). Any l-state energy of the spinless Salpeter equation under the Cornell potential by the WKB approximation method: An application to mass spectra of mesons. *Few-Body Systems, 63*, 6. https://doi.org/10.1007/s00601-021-01705-1

[9] Inyang, E. P., Omugbe, E., Abu-shady, M., et al. (2023). Investigation of quantum information theory with the screened modified Kratzer and a class of Yukawa potential model. *European Physical Journal Plus, 138*, 969. https://doi.org/10.1140/epjp/s13360-023-04617-7

[10] Holevo, A. S. (1998). The capacity of the quantum channel with general signal states. *IEEE Transactions on Information Theory, 44*(1), 269-273.

[11] Hastie, T., Tibshirani, R., & Friedman, J. (2009). *The elements of statistical learning: Data mining, inference, and prediction* (2nd ed.). Springer.

[12] Katz, J., & Lindell, Y. (2014). *Introduction to modern cryptography* (2nd ed.). CRC Press.

[13] Cover, T. M., & Thomas, J. A. (2006). *Elements of information theory.* Wiley-Interscience.

[14] Santana-Carrillo, R., de J. León-Montiel, R., Sun, G.-H., & Dong, S.-H. (2023). Quantum information entropy for another class of new proposed hyperbolic potentials. *Entropy, 25*(1296). https://doi.org/10.3390/e25091296

[15] Bialynicki-Birula, I. (2006). Formulation of the uncertainty relations in terms of the Rényi entropies. *Physical Review A, 74*, 052101. https://doi.org/10.1103/PhysRevA.74.052101

[16] Ikot, A. N., Rampho, G. J., Amadi, P. O., Okorie, U. S., Sithole, M. J., & Lekala, M. L. (2020). Quantum information-entropic measures for exponential-type potential. *Results in Physics, 18*, 103150. https://doi.org/10.1016/j.rinp.2020.103150

[17] Majumdar, S., Mukherjee, N., & Roy, A. K. (2019). Information entropy and complexity measure in generalized Kratzer potential. *Chemical Physics Letters, 716*, 257. https://doi.org/10.1016/j.cplett.2018.12.032

[18] Pooja, A., Sharma, R. G., & Kumar, A. (2017). Quantum information entropy of modified Hylleraas plus exponential Rosen Morse potential and squeezed states. *International Journal of Quantum Chemistry, 117*(11), e25368. https://doi.org/10.1002/qua.25368

[19] Pooja, K., Kumar, G., Gupta, R., & Kumar, A. (2016). Quantum information entropy of Eckart potential. *International Journal of Quantum Chemistry, 116*, 1413. https://doi.org/10.1002/qua.25197

[20] Inyang, E. P., Okon, I. B., Faithpraise, F. O., William, E. S., Okoi, P. O., & Ibanga, E. A. (2023). Quantum mechanical treatment of Shannon entropy measure and energy spectra of selected diatomic molecules with the modified Kratzer plus generalized inverse quadratic Yukawa potential model. *Journal of Theoretical and Applied Physics, 17*(4), 172340 (1-13). https://dx.doi.org/10.57647/j.jtap.2023.1704.40

[21] Isonguyo, C. N., Oyewumi, K. J., & Oyun, O. S. (2018). Quantum information-theoretic measures for the static screened Coulomb potential. *International Journal of Quantum Chemistry, 118*, 025620.

[22] Jaynes, E. T. (2003). *Probability theory: The logic of science.* Cambridge University Press.

[23] Osobonye, G. T., Okorie, U. S., Amadi, P. O., & Ikot, A. N. (2020). Statistical analysis and information theory of screened Kratzer–Hellmann potential model. *Canadian Journal of Physics.* https://doi.org/10.1139/cjp-2020-0041

[24] Romera, E. (2002). Molecular physics. *Molecular Physics, 35*, 5181.

[25] Dembo, A., Cover, T. M., & Thomas, J. (1991). *IEEE Transactions on Information Theory, 37*, 1501.

[26] Romera, E., Sanchez-Moreno, P., & Dehesa, J. S. (2005). Chemical physics letters. *Chemical Physics Letters, 414*, 468.

[27] Ikot, A. N., Rampho, G. J., Amadi, P. O., Sithole, M. J., Okorie, U. S., & Lekala, M. I. (2020). Shannon entropy and Fisher information-theoretic measures for Möbius square potential. *The European Physical Journal Plus*, *135*(503). https://doi.org/10.1140/epjp/s13360-020-00525-2

[28] Abdelmonem, M. S., Abdel-Hady, A., & Nasser, I. (2017). Scaling behavior of Fisher and Shannon entropies for the exponential-cosine screened Coulomb potential. *Molecular Physics*, *115*, 1480. https://doi.org/10.1080/00268976.2017.1299887

[29] Roope, U., Costa, A. C. S., Nguyen, H. C., & Gühne, O. (2020). *Review of Modern Physics*, *92*, 015001. https://doi.org/10.1103/RevModPhys.92.015001

[30] Vedral, V. (2003). Quantum physics: Entanglement hits the big time. *Nature*, *425*, 28–29. https://doi.org/10.1038/425028a

[31] Romera, E., & Santos, F. L. (2008). Fractional revivals through Renyi uncertainty relations. *Physical Review A*, *78*, 013837. https://doi.org/10.1103/PhysRevA.78.013837

[32] Bergou, J. A., Hillery, M., & Saffman, M. (2021). Quantum information theory. In *Quantum Information Processing* (pp. 239-264). Graduate Texts in Physics. Springer, Cham. https://doi.org/10.1007/978-3-030-75436-5_11

[33] Omugbe, E., Osafile, O. E., Okon, I. B., Okorie, U. S., Suleman, K. O., Njoku, I. J., Jahanshir, A., & Onate, C. A. (2022). The influence of external magnetic and Aharonov–Bohm flux fields on the bound state of Klein–Gordon and Schrödinger equations via SWKB approach. *The European Physical Journal D*, *76*, 72. https://doi.org/10.1140/epjd/s10053-022-00507-2

[34] Omugbe, E., Osafile, O. E., Okon, I. B., Eyube, E. S., Inyang, E. P., Okorie, U. S., Jahanshir, A., & Onate, C. A. (2022). Non-relativistic bound state solutions with α-deformed Kratzer-type potential using the supersymmetric WKB method: Application to theoretic-information measures. *The European Physical Journal D*, *76*, 72. https://doi.org/10.1140/epjd/s10053-022-00395-6

[35] William, E. S., Okon, I. B., Inyang, E. P., Akpan, I. O., Ita, B. I., Nwachukwu, A. N., Onate, C. A., Omugbe, E., Okorie, U. S., Araujo, J. P., & Ikot, A. N. (2023). Quantum description of magnetocaloric effect, thermomagnetic properties, and energy spectra of LiH, TiH, and ScH diatomic molecules under the influence of magnetic and Aharonov–Bohm flux fields with Deng-Fan-screened Coulomb potential model. *Molecular Physics, e2195952.* https://doi.org/10.1080/00268976.2023.2195952

[36] William, E. S., Inyang, S. O., Ekerenam, O. O., Inyang, E. P., Okon, I. B., Okorie, U. S., Ita, B. I., Akpan, I. O., & Ikot, A. N. (2024). Theoretic analysis of non-relativistic equation with the Varshni–Eckart potential model in cosmic string topological defects geometry and external fields for selected diatomic molecules. *Molecular Physics.* https://doi.org/10.1080/00268976.2023.2249140

[37] William, E. S., Okon, I. B., Ekerenam, O. O., Akpan, I. O., Ita, B. I., Inyang, E. P., Etim, I. P., & Umoh, I. F. (2022). Analyzing the effects of magnetic and Aharonov–Bohm flux fields on the energy spectra and thermal properties of N_2, NO, CO, and H_2 diatomic molecules. *International Journal of Quantum Chemistry, e26925.* https://doi.org/10.1002/qua.26925

[38] Mukherjee, N., Roy, S., & Sinha, C. (2019). Study of quantum information measures of the scattering states of a two-dimensional electron gas with a Gaussian impurity in a magnetic field. *Physical Review B, 99*(23), 235435.

[39] Ballesteros, Á., & Herranz, F. J. (2016). Maximally superintegrable systems on spaces of constant curvature: The Coulomb problem on the 2D hyperboloid. *Physics Letters A, 380*(35), 2576–2580.

[40] Li, J., Liu, C., & Shi, Y. (2017). Influence of the Aharonov–Bohm flux on the quantum entanglement and coherence of two Dirac particles. *The European Physical Journal D, 71,* 166.

[41] Tóth, G., & Apellaniz, I. (2014). Quantum metrology from a quantum information science perspective. *Journal of Physics A: Mathematical and Theoretical, 47*(42), 424006. https://doi.org/10.1088/1751-8113/47/42/424006

[42] Ahmed, B., & Mustafa, M. (2024). Fisher information and quantum entropies of a 2D system under a non-central scalar and vector potentials. *Research Square*. https://doi.org/10.21203/rs.3.rs-4402782/v1

[43] Edet, C. O., Ettah, E. B., Aljunid, S. A., Endut, R., Ali, N., Ikot, A. N., & Asjad, M. (2022). Global quantum information-theoretic measures in the presence of magnetic and Aharanov-Bohm (AB) fields. *Symmetry, 14*(976). https://doi.org/10.3390/sym14050976

[44] Edet, C. O., & Ikot, A. N. (2021). Shannon information entropy in the presence of magnetic and Aharanov–Bohm (AB) fields. *European Physical Journal Plus, 136*(432). https://doi.org/10.1140/epjp/s13360-021-01438-4

[45] Edet, C. O., Lima, F. C. E., Almeida, C. A. S., Ali, N., & Asjad, M. (2022). Quantum information of the Aharanov–Bohm ring with Yukawa interaction in the presence of disclination. *Entropy, 24*(1059). https://doi.org/10.3390/e24081059

[46] Balachandran, A. P., Marmo, G., Skagerstam, B. S., & Stern, A. (2013). *Gauge symmetries and fibre bundles: Applications to particle dynamics.* Springer.

[47] Gerry, C. C., & Knight, P. L. (2005). *Introductory quantum optics.* Cambridge University Press.

[48] Gonçalves, L. D., Kuru, Ş., Negro, J., & Nieto, L. M. (2014). Quantum solvability and entanglement dynamics of Pöschl-Teller potentials. *Annals of Physics, 351,* 934–943. https://doi.org/10.1016/j.aop.2014.09.014

[49] Kittel, C. (2004). *Introduction to solid state physics* (8th ed.). Wiley.

[50] Weiss, U. (2012). *Quantum dissipative systems* (4th ed.). World Scientific.

[51] William, E. S., Inyang, E. P., & Thompson, E. A. (2020). Arbitrary l-solutions of the Schrödinger equation interacting with Hulthén-Hellmann potential model. *Revista Mexicana de Física, 66*(6), 730–741.

[52] Akpan, I. O., Inyang, E. P., Inyang, E. P., & William, E. S. (2021). Approximate solutions of the Schrödinger equation with Hulthén-Hellmann potentials for a quarkonium system. *Revista Mexicana de Física, 67*(3), 482–490. https://doi.org/10.31349/RevMexFis.67.482

[53] Duan, Y., Li, X., Chang, C., & Zhao, Z. (2022). Calculation of linear and nonlinear optical properties of spherical quantum dots with Hulthén plus Hellmann confining potential. *Optik, 261,* 169187. https://doi.org/10.1016/j.ijleo.2022.169187

[54] Chang, C. (2022). Third-harmonic generation investigated by spherical quantum dot system with Hulthén-Hellmann potential. *Journal of Luminescence, 251,* 119181. https://doi.org/10.1016/j.jlumin.2022.119181

[55] Chang, C., & Li, X. (2022). Second-order nonlinear optical response of tunable GaAs/AlηGa1−ηAs quantum dot with Hulthén-Hellmann potential. *Physica B: Condensed Matter, 645,* 414251. https://doi.org/10.1016/j.physb.2022.414251

[56] Inyang, E. P., Faithpraise, F. O., Amajama, J., William, E. S., Obisung, E. O., & Ntibi, J. E. (2023). Theoretical investigation of meson spectrum via exact quantization rule technique. *East European Journal of Physics, (1),* 53-62.

[57] Ibekwe, E. E., Emah, J. B., Inyang, E. P., & Akpan, A. O. (2022). Mass spectrum of heavy quarkonium for combined potentials (modified Kratzer plus screened Coulomb potential). *Iranian Journal of Science and Technology, Transactions A: Science, 46*(6), 1741–1748.

[58] Eyube, E. S., Makasson, C. R., Omugbe, E., Onate, C. A., Inyang, E. P., Tahir, A. M., ... & Najoji, S. D. (2024). Improved energy equations and thermal functions for diatomic molecules: A generalized fractional derivative approach. *Journal of Molecular Modeling, 30*(12), 1–18.

[59] Inyang, E. P., William, E. S., Ibanga, E. A., Ntibi, J. E., & Akintola, O. O. (2022). Bound state solutions to the Schrödinger equation for selected diatomic molecules. *The Journals of the Nigerian Association of Mathematical Physics, 64,* 1–12.

[60] Inyang, E. P., Ali, N., Endut, R., Rusli, N., & Aljunid, S. A. (2024). The radial scalar power potential and its application to quarkonium systems. *Indian Journal of Physics,* 1–10.

[61] Thompson, E. A., Inyang, E. P., & William, E. S. (2021). Analytical determination of the non-relativistic quantum mechanical properties of near doubly magic nuclei. *Physical Sciences and Technology*, *8*(3-4), 10–21.

[62] Obu, J. A., William, E. S., Akpan, I. O., Thompson, E. A., & Inyang, E. P. (2020). Analytical investigation of the single-particle energy spectrum in magic nuclei of 56Ni and 116Sn. *European Journal of Applied Physics*, *2*(1).

[63] Inyang, E. P., Ayedun, F., Ibanga, E. A., Lawal, K. M., Okon, I. B., William, E. S., ... & Obisung, E. O. (2022). Analytical solutions of the N-dimensional Schrödinger equation with modified screened Kratzer plus inversely quadratic Yukawa potential and thermodynamic properties of selected diatomic molecules. *Results in Physics*, *43*, 106075.